

Solvent Concentration Measurement for Spin Coating

J. GU, M. D. BULLWINKEL, and G. A. CAMPBELL*

Polymer Fabrication and Properties Laboratory, Department of Chemical Engineering, Clarkson University, Potsdam, New York 13699

SYNOPSIS

Planarization of spin-coated polymer films is of great importance for the lithographic process in the microelectronic industry. Solvent retention is an important factor for determining the coating profile during spinning. In this research, solutions of polystyrene in toluene are spin-coated. The coating concentration during spinning is measured on-line using a laser interferometry technique. The optical measurement is evaluated by an off-line gel permeation chromatograph technique. The experiments indicate that a smooth coating surface is required to use the optical method for concentration measurement. The optical technique also provides information regarding the coating surface structure during spinning.

© 1995 John Wiley & Sons, Inc.

INTRODUCTION

Spin coating is used in the microelectronic industry during the lithographic process to produce thin and uniform polymer films on silicon wafers. A puddle of the polymer solution is first deposited on a silicon wafer. The wafer is then accelerated to several thousand rotations per minute (rpm). The coating thickness decreases due to the simultaneous action of solution spin-off and solvent evaporation during spinning. The coating viscosity increases rapidly as the solvent evaporates until the coating becomes so viscous that spin-off stops and the film thins solely by solvent evaporation. Finally, a dry and uniform coating of about 1 micron thickness is left on the wafer. The process usually lasts for tens of seconds.

Often, there is topography on the substrate. In this case, a planar coating surface is required on top of the uneven substrate. The concentration of solvent within the coating might play an important role in coating planarization. The coating profile during spinning is determined by the simultaneous action of centrifugal force, capillary force, viscous force, and solvent evaporation. Leveling of the coating surface is enhanced by the coating surface tension and surface curvature and is retarded by the

coating viscosity. The coating viscosity is a strong function of coating concentration. To investigate the effects of solvent selection and operating conditions on coating planarization, it is necessary to know the solvent concentration in the film during spinning. One potential approach to accomplish this is modeling. However, rheological and diffusion data for many polymer-solvent systems used in the microelectronic industry are often not available in the literature and measurement of these properties is very time-consuming. A measurement technique is therefore of practical importance.

In this article, we describe two techniques for measurement of average solvent concentration in the film during spinning. A laser interferometry technique is used for on-line measurement. An off-line gel permeation chromatography (GPC) technique is performed to evaluate the optical method. The accuracy and limitations of the optical technique are discussed. The optical technique is also used to analyze the coating surface structure during spinning.

MEASUREMENT METHODS

Optical Measurement

Laser Interferometry

Laser light has a very long coherent length, so it can be used for evaluation of thick films. Laser interferometry has been used for many applications in the

* To whom the correspondence should be addressed.

microelectronic industry for on-line measurement.¹⁻³ It was reported, also, to be used for measuring thickness for spin-coating.⁴ In this work, we illustrate the application of laser interferometry to measure the coating refractive index, which, in turn, can be used to estimate changes in coating concentration.

There are many literature data for the refractive index of polymer solutions in the low polymer concentration range.⁵ The solution refractive index can be described by the weighted summation of the refractive index of individual components in a system such as polystyrene (PS) and toluene. The spin-coating process can be approximated as an isothermal process⁶; therefore, the refractive indexes at room temperature are used. The refractive index of PS, toluene, and a silicon wafer are 1.60, 1.49, and 3.82, respectively.⁷⁻⁹

A schematic diagram of the experimental apparatus is shown in Figure 1. The coating is illuminated by the laser beam and the reflected laser beam is received by an optical detector. A PS-toluene solution is spin-coated on a silicon wafer. The coating thickness decreases during spinning due to both solution spin-off and solvent evaporation. Interference intensity changes as coating thickness changes. Figure 2 shows a typical interferogram. This wave provides two types of information: peak-valley magnitude and peak-peak distance. The peak-valley amplitude is determined by the average coating refractive index and the refractive index gradient across the coating thickness. The peak-peak distance is determined by the average coating refractive index and the rate of coating thickness change.

A 1 mW He-Ne (Uniphase) unpolarized laser, 632.8 nm wavelength, is used in this experiment. An incident angle of 7° is used, so normal incidence can be approximated, because the reflection coefficient approaches a constant at small incident angles. The reflected light is measured using a silicon photodiode detector, PIN-10DP (UDT). A Tektronix 2211 os-

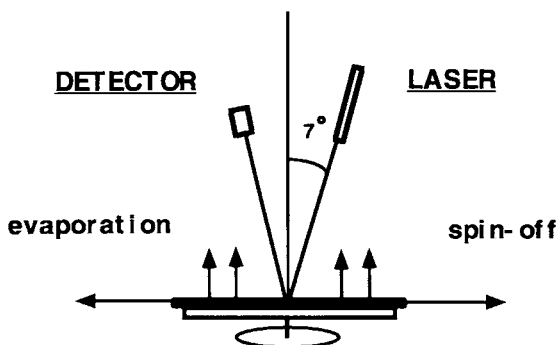
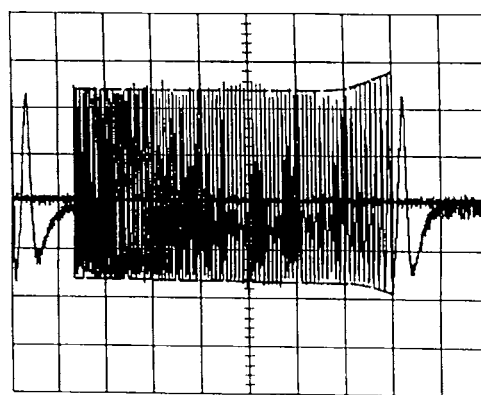
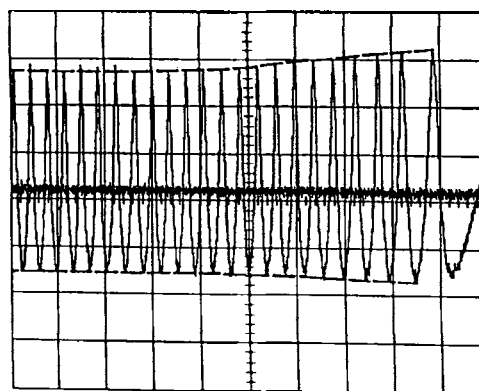


Figure 1 Spin coating and laser interferometer setup.



2s
Whole Process



0.5s

Last Five Seconds

Figure 2 Interferogram for coating 10% solution at 1000 rpm.

cilloscope is used to record the output voltage. Since the range of voltage change in the detector output voltage is only 10 mV during this process compared with the detector output range of 0–1.0 V, the voltage is thus expected to be linear within this small range. The signal is collected in the alternate current (ac) mode, because a much larger scale can be used than in the direct current (dc) mode. However, the low-frequency components will be filtered out in the ac mode. To determine the frequency below which the filter starts to take effect, silicon oil, a nonvolatile fluid which has a constant refractive index, was spin-coated and the output was analyzed. The wave amplitude began decreasing at a frequency below 1.7 Hz, which corresponded to the filter starting frequency. So, the wave collected in the ac mode can be used for quantitative purposes at a signal frequency higher than 2 Hz in this investigation.

Optical Principle

The silicon wafer used as the coating substrate can be considered as a semi-infinite medium.⁷ Interference occurs only at the polished surface. Light reflected from the unpolished side is scattered and, therefore, is negligible. The reflectance of light from a thin film, R , is expressed in terms of Fresnel reflection coefficients and the path difference as follows¹⁰:

$$R = rr^* \quad (1)$$

$$r = \frac{r_1 + r_2 \exp(-2i\delta)}{1 + r_1 r_2 \exp(-2i\delta)} \quad (2)$$

$$\delta = \frac{2\pi n d \cos \varphi}{\lambda} \quad (3)$$

r^* is the conjugate of r ; δ , the path difference; n , the coating refractive index; φ , the incident angle; d , the coating thickness; and λ , the laser wavelength. r_1 and r_2 are Fresnel reflection coefficients at the air-coating and coating-wafer interfaces, respectively. At normal incidence, the extrema of eq. (1) occurs at

$$\delta = \frac{\pi}{2} m \quad (4)$$

m is an integer number. As m equals an even and odd number, extrema R_1 and R_2 are, respectively,

$$R_1 = \left(\frac{n_s - 1}{n_s + 1} \right)^2 \quad (5)$$

$$R_2 = \left(\frac{n_s - n^2}{n_s + n^2} \right)^2 \quad (6)$$

n_s is the substrate refractive index. Whether R_1 corresponds to the maximum or minimum reflectance depends on whether n_s is larger or smaller than n . In our case, the silicon wafer has a larger refractive index than that of the coating; therefore, R_1 and R_2 are the maximum and minimum reflectance, respectively, and R_1 is equal to the uncoated wafer reflectance. The coating refractive index is derived by the envelope method, by neglecting the absorption index.¹¹ The envelope method was originally developed for spectrometer measurements, where the film thickness was a constant and the wavelength was a variable. When applying the envelope method to the laser interferometer, the thickness is time-dependent and the wavelength is fixed. Con-

necting maximum and minimum extrema in Figure 2, R_1 and R_2 , upper and low envelopes of extrema, are now a continuous function of time and are represented by eqs. (5) and (6). From the ratio of R_2 over R_1 , n is determined by

$$n = \left(\frac{\frac{n_s + 1}{n_s - 1} - \left(\frac{R_2}{R_1} \right)^{1/2}}{\frac{n_s + 1}{n_s - 1} + \left(\frac{R_2}{R_1} \right)^{1/2}} \right)^{1/2} \quad (7)$$

n is a continuous function of time, changing during spinning. The coating thickness change, Δh , between any two peaks is given by

$$\Delta h = \frac{\lambda}{2(n^2 - \sin^2 \varphi)^{1/2}} \quad (8)$$

The accuracy of this optical measurement is affected by three major factors. One is the noise due to rotation. The laser beam may not be perfectly focused on the rotating axis and has a defined area; it is not a point source. A bare uncoated wafer will produce a background noise during spinning. This noise will be superimposed on the envelopes. The second factor is the diffusion caused by a concentration gradient across the coating. A uniform coating concentration is assumed in the above equations. Without proper knowledge of the concentration profile, errors will be introduced by assuming a uniform coating. A laser is a single wavelength light source and provides only one data point at one time. Therefore, it is not possible to explore both average concentration and concentration gradient simultaneously. Rapid scan spectrometers have the ability to catch both pieces of information. However, the spectrometer has only a very short coherent length, so it cannot be used for the thick films in this work. For a positive gradient, i.e., the refractive index increases from substrate to coating surface, the actual wave amplitude is larger than that calculated by assuming a uniform coating when n_s is larger than n . For a negative gradient under the same condition, the actual amplitude is smaller than that of assuming a uniform coating. Figure 3 shows the computer-simulated interferogram for cases of the same average refractive index but different linear refractive index gradients. n_a and n_s are the coating refractive index at the air-substrate boundary. The substrate is a silicon wafer. A difference in amplitude is predicted. It is also observed that the wave frequency depends only on the average refractive index, not on its gradient. It can be shown that the wave am-

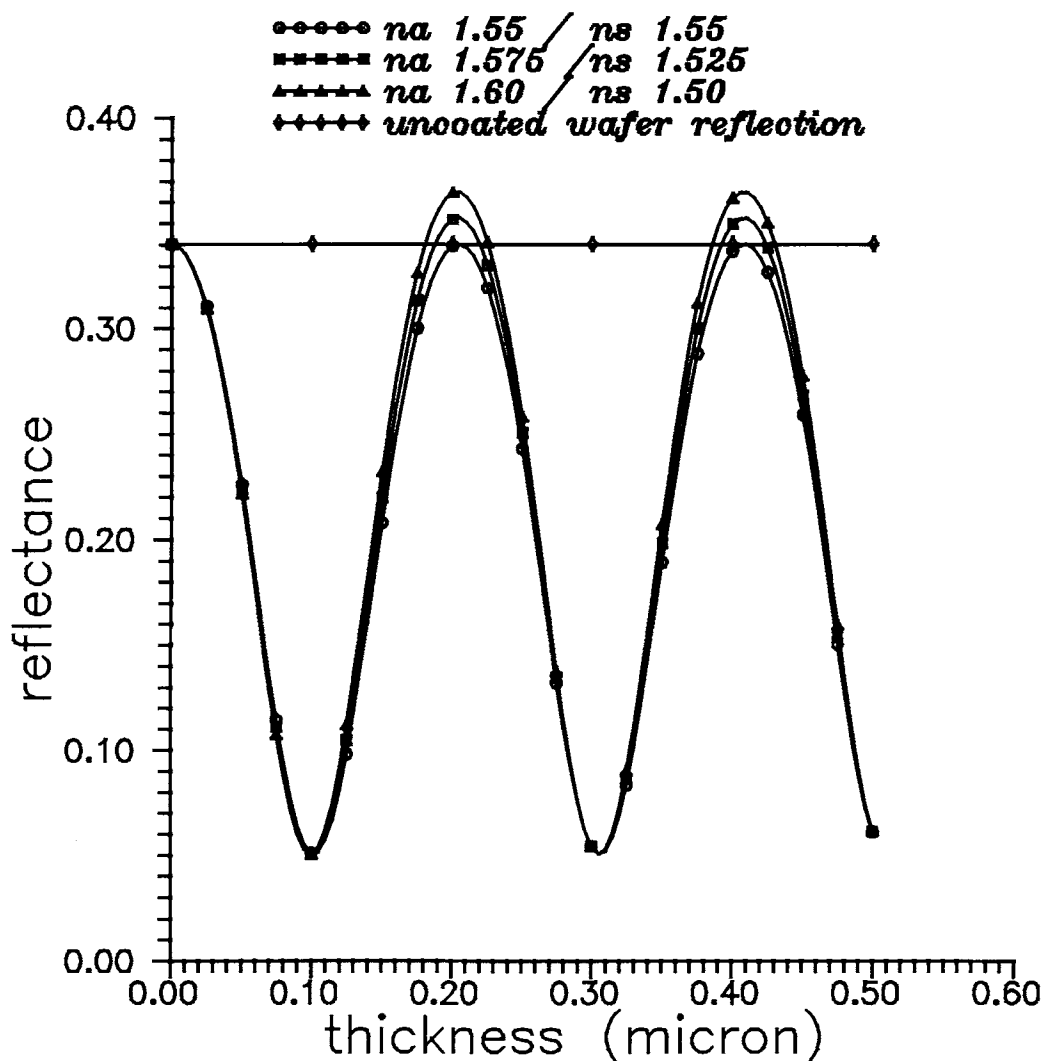


Figure 3 Effect of refractive index gradient on interference wave amplitude.

plitude difference depends not only on the concentration gradient, but also on the difference of the refractive index between coating and substrate. The smaller this difference, the larger the difference in wave amplitude. A high refractive index substrate should be selected to reduce the effect of the concentration gradient effect. A larger difference in wave amplitude than those observed in Figure 3 is expected if quartz is used as the substrate, because quartz has a refractive index very close to that of the coating. The third factor concerns the conditions at the air-coating boundary. Because there is spin-induced air flow and solvent evaporation above the coating surface, the air-coating boundary may not be optically sharp. The magnitude of the error introduced by this factor is difficult to quantify analytically.

GPC Concentration Measurement

Average coating concentration is measured by analyzing the samples of the wet films after spin-coating the wafers at different amounts of time. For the off-line measurement, the major limitation of this method is that the solvent continues to evaporate after spinning. Error will be introduced by delay of the measurement. This difficulty is minimized by placing the coated wafer into a second solvent. The coating solvent concentration in the second solvent is very low and the evaporation loss is negligible. The coating solvent is then "trapped" within the second solvent. After the coating is dissolved, the solution is analyzed to give the ratio of the polymer to the coating solvent, i.e., the coating concentration.

GPC has been used to analyze the low molecular weight component in plastics. By selecting a column with small pore size, the polymer will be eluted as a single narrow peak at the exclusion limit and the solvent will be eluted at a later time. GPC has a very stable base line. With a UV detector, a 0.5% relative standard deviation can often be achieved.¹² In this work, a Waters GPC 150C is used, connected to a Waters 484 UV detector, set at a 254 nm wavelength. A Waters Ultrastaygel 100 Å column is selected and tetrahydrofuran (THF) is adopted as a mobile phase. A 125 mm (5 in.) wafer was spin-coated. The coated wafer spun at different amounts of time is immediately transferred to a Pyrex dish, filled with 50 mL THF solvent, which is the same solvent used as the GPC mobile phase to avoid a polymer-chain configuration change in the GPC mobile phase. The solution is then sampled with a syringe and the sample is analyzed using GPC.

SPIN COATING EXPERIMENTAL

The polystyrene used in this investigation has a reported M_w of 310,000 and M_w/M_n of 3.1. The spin-coater (Solid State Corp. 140), set at full acceleration and brake, was set for different spin times. Spin speed was set at 1000 ± 5 rpm, calibrated by an optical tachometer. A special lightweight aluminum chuck was built to reduce the system inertia. Acceleration and brake periods were not observed at this spin speed, which reduced the off-line error. It took about 2 s to move the coated wafer to the THF solvent. The solvent lost within this period was found to be small compared with the amount of the solvent remaining within the coating. So, the error caused by this delay was small. Dry coating thicknesses were measured using a DEKTAK IIA (Sloan) profilometer.

RESULTS AND DISCUSSION

Eight and ten weight percent PS solutions were spin-coated at 1000 rpm, which gave 1.2 and 1.8 μm dry coating thicknesses, respectively. Figure 2 is the interferogram for coating a 10% solution, with the bare wafer rotation noise recorded at the center. The time scale in Figure 2 is 2 and 0.5 s for the whole process and the last 5 s period, respectively. In this case, the process lasts 16 s.

The dc wave is required to calculate the coating refractive index. The following procedure is used to convert the recorded ac envelopes in Figure 2 to the

dc envelopes in Figure 4. Since n_s is larger than n , the bare wafer reflectance R_1 is the maximum reflectance—a constant. So, the dc upper envelop in Figure 4 is a straight line. Thus, the upper envelop coordinate f , a constant, is determined by

$$\frac{R_2}{R_1} = \frac{f - \Delta f}{f} \quad (9)$$

Δf is the difference between the upper and low envelopes at zero spin time in Figure 2. R_1 and R_2 are given by eqs. (5) and (6) for the initial coating solution concentration. The low envelope coordinate is determined by subtracting the wave amplitude in Figure 2 from the upper envelop. Then, a continuous n is obtained through applying eq. (7). The final n calculated from Figure 4 is 1.66, 4% higher than 1.60 of PS. It is an unrealistic value, resulting from the errors discussed above. The amplitude of last peak in Figure 2 is smaller than that of the other peaks. This peak is partially filtered, because its frequency is lower than 2 Hz, as seen from the time coordinate in Figure 2. The concentration at the last peak is determined by adding the solvent mass corresponding to the last peak, using eq. (8), to the 1.8 μm drying coating, because there is no solvent spun off the substrate at this polymer concentration. The laser can only provide information when the coating thickness is changing. Therefore, we are not able to determine the coating concentration at the end of spinning, at an essentially constant thickness. A completely dry coating after spinning is assumed here for simplification. The obtained concentration at the last peak is 87%. The n calculated from the

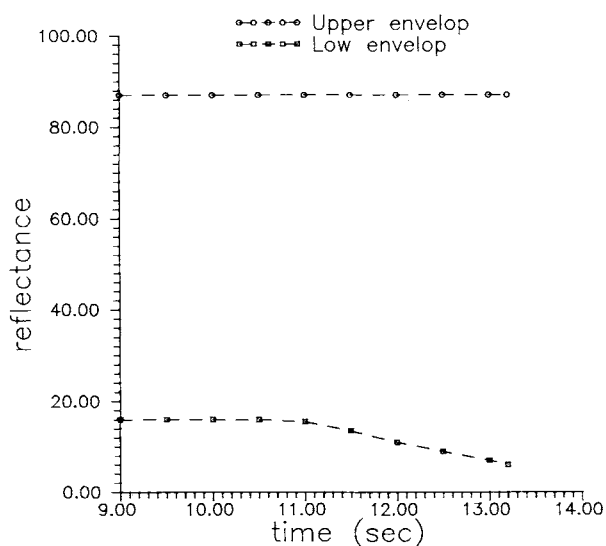


Figure 4 dc interference envelopes.

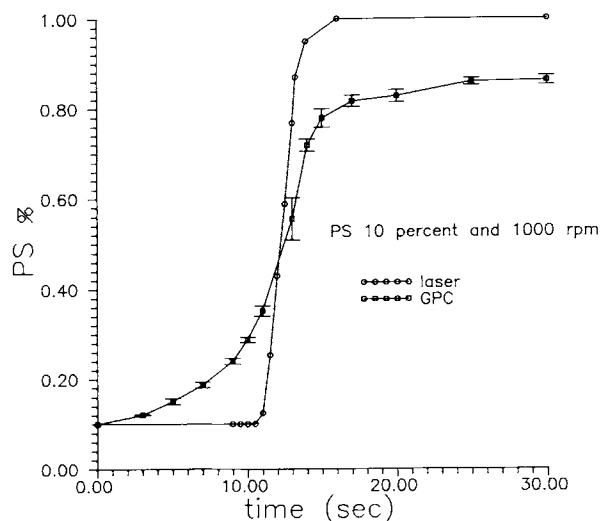


Figure 5 GPC and laser-measured concentration for coating 10% solution at 1000 rpm.

envelopes is then linearly reduced to match the 87% at the last peak. The results are plotted in Figure 5.

The GPC measured concentration is also shown in Figure 5 for comparison. The GPC curve can be approximated by two line segments. The first line lies from 0 to 10 s, having a smaller slope. The second line, starting from about 30% PS, has a larger slope. The optical measurement is not sensitive to the small slope. It only responds to the large slope and correlates with the inflection point of change in concentration with time from the GPC data. It can be shown that the errors caused by rotation noise and concentration are no more than 10% in this case. Therefore, the major cause of the error is probably that the air-coating boundary is not optically sharp. Figure 6 is for coating an 8% solution, and a similar relationship is observed.

The optically measured concentrations for coating four different concentration solutions are illustrated in Figure 7. The spin speed is 1000 rpm for all cases. The dry coating thicknesses are 0.25, 1.2, 1.8, and 2.7 μm , corresponding to different initial coating solution concentrations. Using the two-segment assumption, we know that (1) the optical measurement response starts from about 30% PS and small concentration change information is lost. Thus, the optical measurement is only qualitative for a single case, and (2) the distance between these curves, corresponding to the inflection points with the concentration time function, thus provides a quantitative comparison of solvent retention. Therefore, this technique may be used as an efficient quantitative comparison of the effects of solvent selection and operation condition on coating solvent concen-

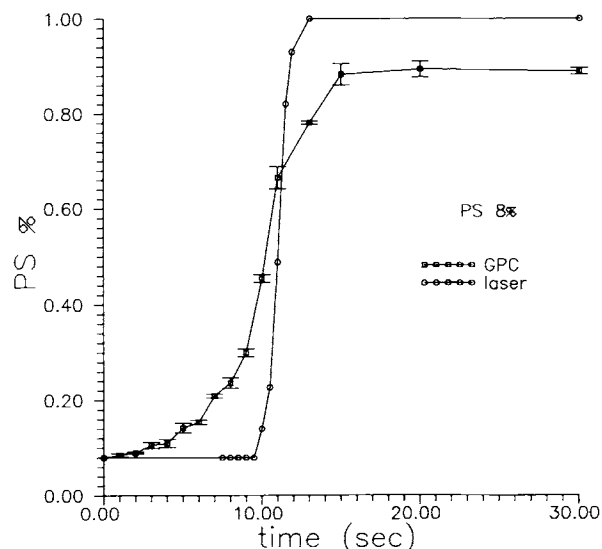


Figure 6 GPC and laser-measured concentration for coating 8% solution at 1000 rpm.

tration during spinning. If more detail in the concentration time function is required, then the GPC technique would be indicated.

We are not able to apply the optical technique to PS-methyl ethyl ketone (MEK) and PS-chloroform systems. Figure 8 shows the profilometer measurements for the PS dry coating surface coated with PS-toluene and PS-MEK solutions. The deep trench in the figure is razor-cut for coating thickness measurement. A smooth coating surface is achieved with the toluene solution and a rough surface is ob-

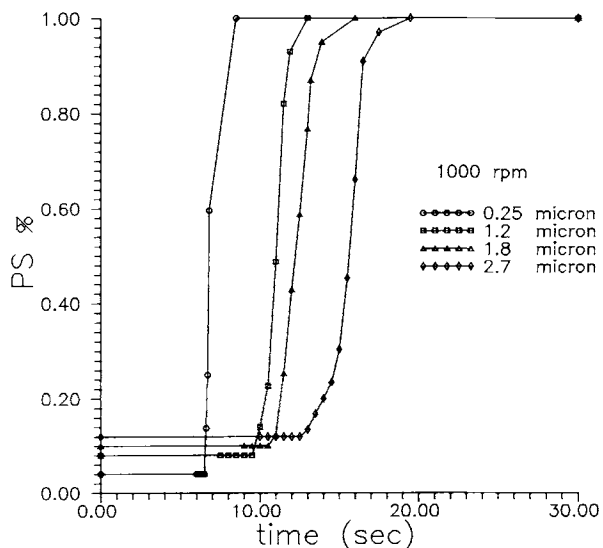


Figure 7 Laser-measured concentration at 1000 rpm for four different dry thickness coatings.

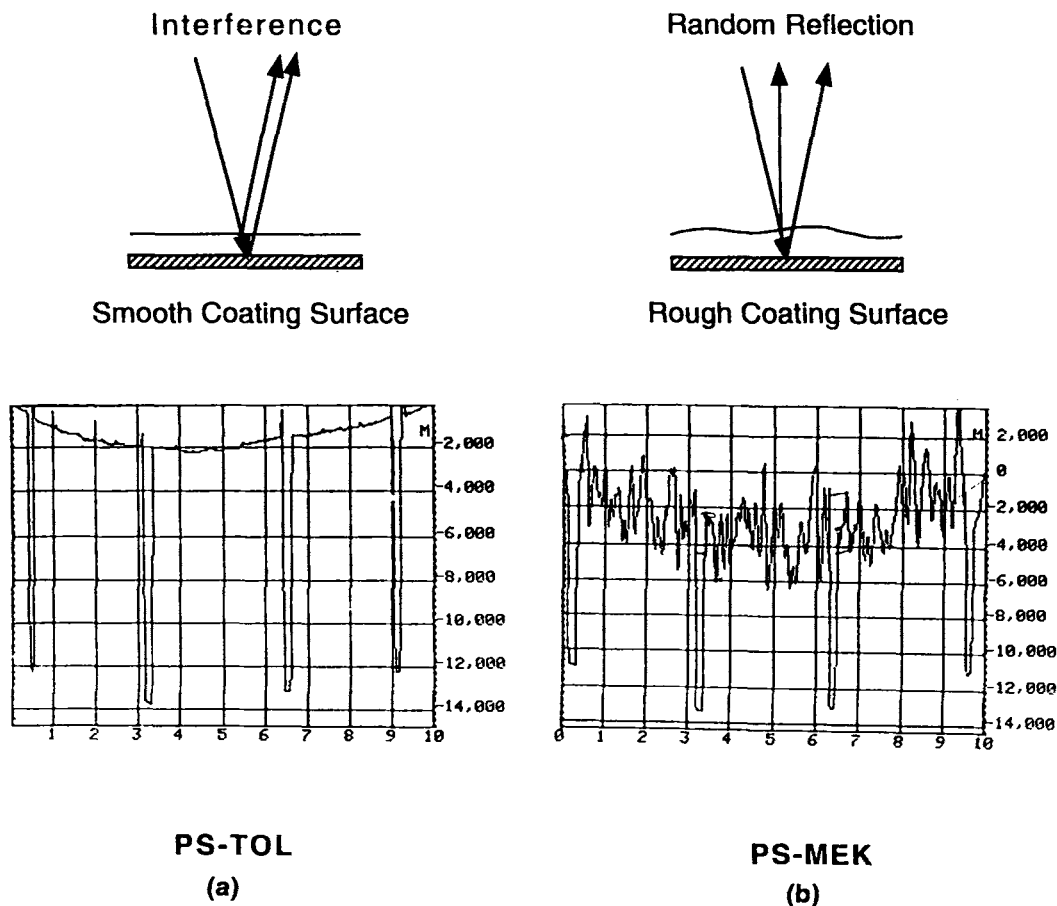


Figure 8 PS coating surface: (a) PS-toluene; (b) PS-MEK.

served for the MEK solution. Similar roughness is also observed with the PS-chloroform solution-coated surface. Light is scattered on the rough surface. A smooth coating surface is a prerequisite for the lithographic purpose. Any solvent corresponding to a rough surface will be excluded for further investigation. Therefore, a rough coating surface should not become a problem for applying this technique in the microelectronic industry.

The causes of spin-coated film roughness have been related to rapid solvent evaporation,¹³ flow instability,¹⁴ and poor solvent¹⁵ in the literature. However, all the explanations were based on observation of the drying coating surface after spinning, not during spinning. Interference or scattering is related to a smooth or rough surface. Therefore, the interference technique provides direct surface information during spinning. If there is a transition from a smooth to a rough coating surface during spinning, a corresponding transition from interference to a scattering pattern could be expected to be observed.

Figure 9(a) is the interferogram of spinning only the MEK solvent. An interference wave is observed, which corresponds to a smooth surface during spinning. However, only random reflections are observed for spinning a PS-MEK solution [Fig. 9(b)]. The surface is optically rough from the start. A similar phenomenon was also observed for coating a chloroform solvent and a PS-chloroform solution. Both MEK and chloroform solvents have a higher evaporation rate than that of MEK and the chloroform solutions, respectively, but the solvent surface is smooth and the solution surface is rough during spinning. Sparrow and Gregg suggested the mass transfer coefficient k_s for a rotating disk¹⁶:

$$m = aMW_s p_i \Omega^{1/2} \quad (10)$$

a is a constant, MW_s and p_i are solvent molecular weight and solution vapor pressure, respectively, and Ω is the spin speed. The evaporation rate is proportional to the product of the solvent molecular weight and vapor pressure. The three solvents used, toluene,

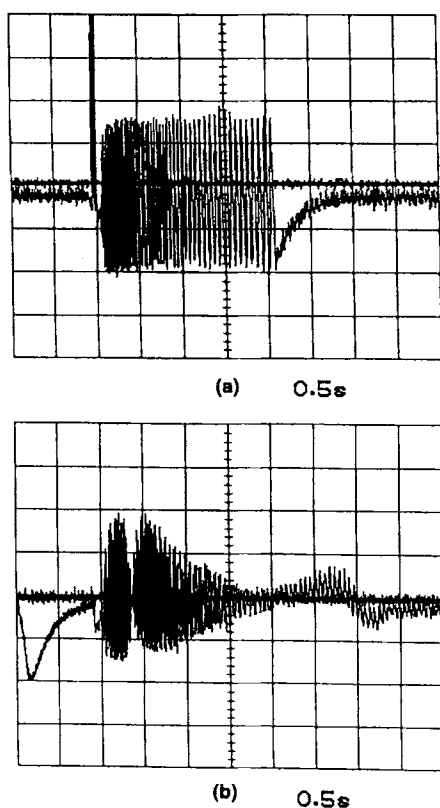


Figure 9 Surface information during spinning: (a) MEK solvent; (b) PS-MEK solution.

MEK, and chloroform, have a ratio of this product of 1:3:9, respectively, at room temperature. The evaporation rate can be adjusted by the spin speed. By spinning the PS-toluene solution at high speed and PS-MEK and PS-chloroform solutions at low speed, the same evaporation rate can be achieved. Still under these conditions a rough surface was observed for MEK and chloroform solutions and a smooth surface for the toluene solution both during spinning and after spinning. Apparently, the rough coating surface cannot be explained by considering the evaporation rate only.

There is no fundamental difference in the coating flow pattern between spinning the MEK solvent and MEK solution; the stability theory therefore appears not a proper explanation for the very different surface phenomena during spinning. The exponent in the Mark-Houwink equation, associated with the goodness of the solvent and used by Spangler et al.,¹⁴ is 0.73 for both toluene and chloroform, so it also cannot be applied as a criterion for the difference between coating roughness of the systems as suggested in the literature.

Surface roughness is often referred to as orange peel and crater in the literature. The coating surface

is not leveled in this case. This surface phenomenon is often explained by the Marangoni effect, a surface tension gradient-driven vortex under the coating surface.¹⁷ Benard cells on the coating surface corresponding to the vortex can be observed under a microscope. However, a rough coating surface is not always observed. The surface tension of toluene, MEK, and chloroform are 28, 25, and 27 dyn/cm, respectively.¹⁸ A dramatic difference of surface phenomena both during spinning and after spinning thus cannot properly be explained by a minor difference of pure solvent properties under the same evaporation rate.

Thermodynamics of the solution might be used to explain the observed surface phenomena. Without chemical reaction, mixing or dissolving is an endothermic process.¹⁹ The process approaches athermal if two components have a similar structure, which corresponds to the maximum negative Gibbs free-energy change, ΔG :

$$\Delta G = \Delta H - T\Delta S \quad (11)$$

ΔH and ΔS are mixing enthalpy and entropy, respectively. If two components are significantly different in structure, the required ΔH is so large that ΔG may become positive. In this case, dissolving is unfavorable. The closer the structure between the polymer and solvent, the better the dissolving characteristic.

Coating drying is opposite to the dissolving process. The polymer has a stronger tendency to be phase-separated in a solvent with a different structure than in a solvent with a similar structure at the same condition. Contrary to dissolving, demixing is an exothermic process. During drying, polymer-solvent contact is replaced by polymer-polymer contact, which is accompanied by an energy release and constitutes the thermal driving force. This molecular level thermal driving force may also contribute to the vortex within the coating, together with the surface tension gradient driving force. For toluene, the thermal driving force is negligible because of the minimum of dissolving enthalpy. For MEK, a large thermal driving force is expected. From this point, the difference of thermodynamics between the solvents investigated is significant.

Polymer solution drops were observed under a microscope for understanding the effect of the surface tension gradient on surface phenomena. For the PS-MEK solution drop, an intense vortex and the accompanied Benard cell was observed, which corresponds to a rough dry coating surface, while only an extremely weak Benard cell was noticed for

the PS-toluene solution drop, which corresponds to a smooth dry coating surface. The PS-chloroform solution drop falls between these extremes. The observations both during spinning using a laser interferometer and under a microscope indicate that factors other than the surface tension gradient might be introduced. Possibly, the matching of polymer and solvent structure, corresponding to a minimum dissolving enthalpy, will reduce the thermal driving force and a smooth surface might be expected.

CONCLUSION

The concentration in PS-toluene solution spin-coated film was studied by GPC and optical methods. The GPC technique provides quantitative measurement. The optical measurement was found to indicate the inflection point of the concentration curve but was not sensitive to a small concentration change. The optical measurement was thus qualitative for a single case, but can provide quantitative comparison when different cases are studied and would be a useful screening technique. A rough coating surface was observed when MEK and chloroform solvent were used. A coating surface during spinning was analyzed by an optical method. The results indicate that the spin-coated film roughness could not be properly described by the current literature explanation. Solution thermodynamics is suggested as a possible factor to explain the observed surface phenomena.

This research was partially supported by IBM Corporation, Essex Junction Vermont Division. The authors are very grateful for the support.

REFERENCES

1. K. L. Saenger and H. M. Tong, *J. Appl. Polym. Sci.*, **33**, 1777 (1987).
2. H. H. Busta, R. E. Lajos, and P. A. Kiewit, *Solid State Technol.*, **Feb.**, 61 (1979).
3. P. D. Krasicky, R. J. Groele, and F. Rodriguez, *Chem. Eng. Commun.*, **54**, 1279 (1987).
4. L. M. Peurrung and D. B. Graves, *J. Electrochem. Soc.*, **138**, 2115 (1991).
5. M. B. Huglin, *J. Appl. Polym. Sci.*, **9**, 3963 (1965).
6. P. C. Sukaneck, *J. Image. Tech.*, **11**, 184 (1985).
7. T. Huen, *Appl. Opt.*, **18**, 1927 (1979).
8. J. Brandrup and E. H. Immergut, Eds., *Polymer Handbook*, Wiley, New York, 1989.
9. R. C. Weast, Ed., *Handbook of Chemistry and Physics*, CRC Press, Boca Raton, FL, 1986.
10. O. S. Heavens, *Optical Properties of Thin Solid Films*, Dover, New York, 1965.
11. D. B. Kushev, N. N. Zheleva, Y. Demakopoulou, and D. Siapkas, *Infrared Phys.*, **26**, 385 (1986).
12. D. Noel, K. C. Cole, and J. J. Hechler, *J. Chromatogr.*, **408**, 129 (1987).
13. J. H. Lai, *Polym. Eng. Sci.*, **19**, 1117 (1971).
14. L. L. Spangler, J. M. Torkelson, and J. S. Royal, *Polym. Eng. Sci.*, **30**, 644 (1990).
15. B. Reisfeld, S. G. Bankoff, and S. H. Davis, *J. Appl. Phys.*, **82**, 294 (1960).
16. E. M. Sparrow and J. L. Gregg, *J. Heat Transfer*, **82**, 294 (1960).
17. F. J. Hahn, *J. Paint Tech.*, **43**, 58 (1971).
18. M. Grayson and D. Eckroth, Eds., *Encyclopedia and Chemical Technology*, Wiley, New York, 1981.
19. M. Kurata, *Thermodynamics of Polymer Solutions*, Harwood, NY, 1982, p. 60.

Received October 20, 1994

Accepted January 19, 1995